

Gauri D. Bajju*, Sapna Katoch, Gita Devi, Sujata Kundan, Ashu and Madhullika Bhagat

Synthesis and characterization of some new thallium(III) macrocyclic complexes and their biological studies

DOI 10.1515/mgmc-2015-0027

Received August 31, 2015; accepted February 8, 2016; previously published online April 22, 2016

Abstract: New symmetrically *para*-substituted tetraphenylporphyrin Tl(III) salicylate complexes, having the general formula SA/5-SSATl(III)t(4-Y)PP (Y=-H, -CH₃, -OCH₃); SA=salicylates and 5-SSA=5-sulfosalicylates, were synthesized and characterized by elemental analysis, optical absorption/emission studies, infrared spectrum, NMR studies (¹H, ²⁰⁵Tl), thermal analysis and mass spectra; the complexes are in good consistency with experimental results. All the newly synthesized complexes exhibited good optical property, and thermogravimetric analysis (TGA) results showed their excellent thermal stability (>400°C). Macrocyclic complexes of Tl(III) ligate to axial ligand to form six-coordinate complex, the nature of which influences the photophysical properties of the former depending upon the spin-orbital coupling character of the axial ligand. A square-based pyramidal structure has been proposed on the basis of these studies. In addition, some of the synthesized complexes of thallium porphyrins were also screened for anti-bacterial activity. Cytotoxic activity of 5-SSATl(III)t(4-OCH₃)PP evaluated against four human cancer cell lines exhibited strong (up to 90%) growth inhibition.

Keywords: antibacterial activity; cytotoxic activity; macrocyclic complexes; salicylates; tetraphenylporphyrins.

Introduction

Tetrapyrrolic macrocycles like porphyrin and phthalocyanines have attracted considerable interest and hold a

special place in modern chemistry functioning as reaction catalysts (Karimipour et al., 2007, 2012, 2013), oxygen transporters, chemical sensors (Cosma et al., 2009; Musturappa et al., 2013), or in molecular electronic devices (Drain et al., 2002). Porphyrins were reported to exhibit a variety of biological activities. This is due to the fact that natural and synthetic porphyrins have relatively low toxicity *in vitro* and *in vivo*, and they possess antitumor (Antonova et al., 2010; Fadda et al., 2013) and antioxidant effects (Stojiljkovic et al., 2001; Yuasa et al., 2007) and have a good potential for ion complexation. The ability for numerous chemical modifications and the large number of different mechanisms by which porphyrins affect microbial and viral pathogens place porphyrins into a group of compounds with an outstanding potential for discovery of novel agents, procedures and materials active against pathogenic microorganisms. Porphyrins with only one, two, or more substituents present a compact architecture that suits a wide variety of applications or further synthetic elaboration. To synthesize porphyrins bearing a molecular recognition site, porphyrin synthons that have functional groups at the *p*-positions of the *meso*-phenyl groups are usually employed, since these functional groups might be further modified by chemical treatments to enhance selectivity in the porphyrin-mediated reactions. Although the coordination of most of the metallic elements to the porphyrin macrocycle has been demonstrated for many years, it was transition-metal porphyrin complexes which were the focus of the most intense attention. More recently, there has been a resurgence of interest in main-group chemistry, driven by the search for new conducting materials and new chemotherapeutic agents and the recent discovery of previously unsuspected bonding modes for main-group elements. Porphyrin complexes of the main-group elements have not been excluded from this renewed interest, and there has been recent activity in the study of elements from groups 13 and 14 coordinated to the porphyrin macrocycle. Gallium(III), indium(III) and thallium(III) porphyrins have been receiving more attention due to their good medical application and non-linear optical (NLO) properties (Rajesh et al., 2010; Fitzgerald

*Corresponding author: Gauri D. Bajju, Department of Chemistry, University of Jammu, New Campus, Baba Sahib Ambedkar Road, Jammu 180 006, India, e-mail: gauribajju@gmail.com

Sapna Katoch, Gita Devi, Sujata Kundan and Ashu: Department of Chemistry, University of Jammu, New Campus, Baba Sahib Ambedkar Road, Jammu 180 006, India

Madhullika Bhagat: School of Biotechnology, University of Jammu, New Campus, Baba Sahib Ambedkar Road, Jammu 180 006, India

et al., 2015). Sn(IV) compounds possessed diversified applications in industries and agriculture and acts as good photosensitizer (Manke et al., 2014). Thallium(III) porphyrins show a range of properties, among the most striking of which is the remarkable structural diversity which differs from typical coordination geometries observed for most metalloporphyrin complexes. Another favorable feature of these complexes is their capability of hosting tri- or tetravalent central atoms that require the further coordination of one and two axial substituents, respectively. In fact, axial substituents indirectly stabilize the electronic excited states which are involved in the multiphoton absorption processes through either preventing or reducing intermolecular aggregation in solution with the increase of molecule concentration. Following the preceding discussion, we have synthesized the series of axially substituted thallium(III) porphyrins.

In particular, we prepared meso-tetraphenylporphyrin (H_2tPP) and its para-substituted derivative $H_2t(4-Y)PP$ ($Y=p-CH_3, p-OCH_3$) aquo-meso-(5,10,15,20-tetraarylporphyrinato)thallium(III)hydroxide, $[(OH)(H_2O)Tl(4-Y)PP]$, axially ligated Tl(III) porphyrins; meso-tetraphenylporphyrinato salicylato thallium(III), $Tl(4-Y)PPSA$ and meso-tetraphenylporphyrinato 5-sulphosalicylatothallium(III), $Tl(4-Y)PP$ 5-SSA. Finally, the biological activity of the newly synthesized porphyrin ligands and their complexes was tested against some Gram (+) and Gram (-) bacteria (*Escherichia coli*, *Pseudomonas fluorescens*, *Staphylococcus aureus* and *Bacillus subtilis*).

Results and discussion

Elemental analysis

All the resulting solids are soluble in $CHCl_3$, CH_2Cl_2 , CH_3OH and DMSO. The analytical data of the complexes of thallium(III) metal complexes are given in Table 1.

Table 2: Optical absorption data of free base porphyrins and their Tl(III) derivatives in different solvents.

Compound	Solvent	B band		Q bands	
		λ_{max} (nm)		λ_{max} (nm)	
H_2tPP	Acetone	422	514, 549, 590, 646,		
	Chloroform	414	512, 546, 592, 644		
$H_2t(4-CH_3)TPP$	Acetone	422	517, 533, 592, 648		
	Chloroform	420	515, 533, 590, 646		
$H_2t(4-OCH_3)PP$	Acetone	422	516, 557, 594, 651		
	Chloroform	420	515, 556, 592, 649		
$(OH)(H_2O)Tl(4-H)PP$	Acetone	438		568, 606	
	Chloroform	438		566, 605	
$(OH)(H_2O)Tl(4-CH_3)PP$	Acetone	449		453, 671	
	Chloroform	447		451, 672	
$(OH)(H_2O)Tl(4-OCH_3)PP$	Acetone	431		518, 568	
	Chloroform	430		517, 566	

Absorption spectroscopy

The B and the Q bands in the spectrum of typical porphyrin both arise from $\pi-\pi^*$ transitions and can be explained by considering the four frontier orbitals (Milgrom, 1997) (HOMO and LUMO orbitals) (the Gouterman four-orbital model). From the UV-Vis absorption values given in the Experimental section, it can be clearly observed that variation of the peripheral substituents on the porphyrin ring causes minor changes in the intensity and wavelengths of these absorptions, and their spectral data in different solvents (Table 2) shows that many of the absorption bands of para-substituted derivatives exhibit bathochromic (red shift) as compared to the unsubstituted porphyrin. The electronic absorption spectra of aquo-meso-tetraaryl porphyrinato thallium(III) hydroxide $(OH)(H_2O)Tl(III)tp$ and $(OH)(H_2O)Tl(III)t(4-Y)PP$, $Y=-CH_3, -OCH_3$ are of normal two-banded type. It is apparent from the spectra that there is no major distortion of the macrocycle ring upon metalation and that the large metal atom is situated above rather than in the plane of the porphyrin ring. Both B bands (350–450 nm) and Q bands (500–700 nm)

Table 1: Analytical data of some of the axially ligated complexes of Tl(III) porphyrins.

Elemental analysis	Calculated percentage				Found percentage			
	C	H	N	S	C	H	N	S
SATltp	62.87	3.60	5.73	0.00	62.36	3.68	5.72	0.00
5-SSATltp	59.04	3.08	5.40	3.08	59.02	3.06	5.48	3.10
SATl(4- CH_3)PP	63.18	3.90	5.36	0.00	63.38	3.73	5.30	0.00
5-SSATl(4- CH_3)PP	60.52	3.75	5.13	2.93	60.23	3.62	5.23	2.74
SATl(4- OCH_3)PP	60.13	3.73	5.10	0.00	60.25	3.69	5.33	0.00
5-SSATl(4- OCH_3)PP	47.6	3.55	4.85	2.77	47.59	3.43	4.78	2.83

were found to be red-shifted in all thallium porphyrins (Figure 1). Also, the molar absorbance of both the main Soret and the Q bands of the metalloporphyrins are higher than the corresponding values for the free-base porphyrin (Tables 2 and 3). According to earlier observations (Horvath et al., 2004, 2006; Valicsek et al., 2004, Valicsek et al., 2011) this type of spectral properties is unambiguously characteristic for OOP (out of plane) or Sat (sitting atop) complexes, confirming the expectations based on the size (95 pm ionic radius) of Tl(III). Not only metalation but also axial coordination is accompanied by red shifts of the characteristic absorption bands. As the corresponding values for B(0,0) itself indicate, the larger OOP distance in case of axially ligated porphyrin results in the higher dome distortion of the porphyrin ligand. For the Q(0,0) band the effect of the axial ligand is much stronger, indicating that the energy of the S_1 state

is more influenced by this structural change. The f values (oscillator strength) of some of the metalated porphyrin and their axially ligated derivatives (Table 3) show that change in polarity of the solvent does not significantly alter the position of transitions but result in an enhanced full width at half maximum (fwhm) (1/2) value indicating weak interactions with the solvent.

The optical absorption spectra of axially ligated Tl(III) porphyrins when recorded in different solvents show only marginal change in λ_{\max} values. The spectrum of the complex SATl(III)t(4-CH₃)PP is shown in Figure 2.

Infrared spectroscopy

The infrared (IR) spectral data of various synthesized complexes of thallium porphyrins are listed in Table 4.

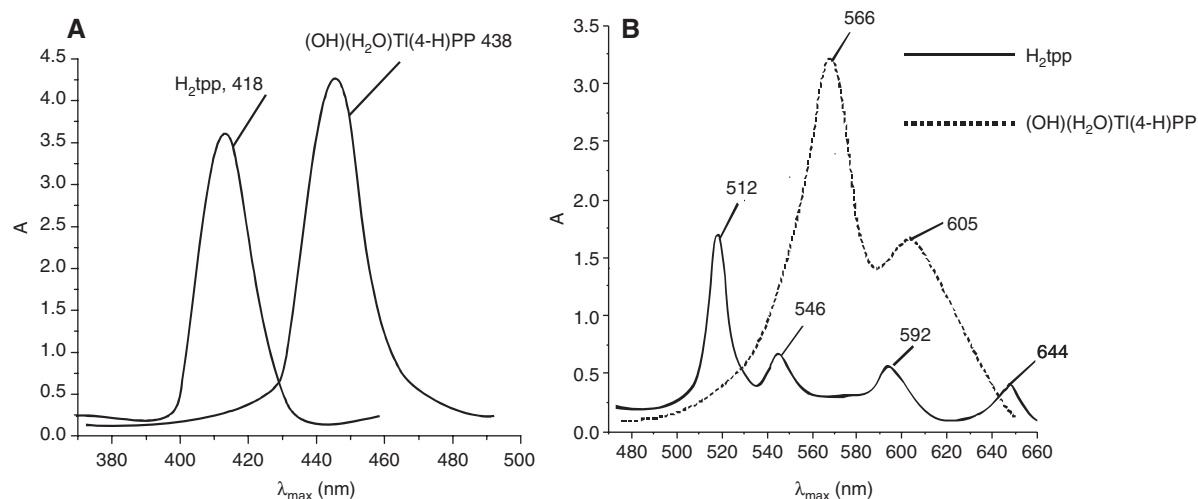


Figure 1: UV visible spectra of free base porphyrin and thallium(III) porphyrin.

(a) UV-visible overlapped B-bands of H₂tpp and (OH)(H₂O)Tltpp. (b) UV-visible overlapped Q-bands of H₂tpp and (OH)(H₂O)Tltpp.

Table 3: Optical absorption data of axially ligated thallium porphyrins in different solvents together with $\log \epsilon$ and $\nu_{1/2}$.

Compound	Solvent	λ_{\max} , nm ($\log \epsilon$, M ⁻¹ cm ⁻¹)			$\nu_{1/2}$ (cm ⁻¹)		$F=4.33 \times 10^{-9} \epsilon \Delta \nu_{1/2}$	
		B(0,0)	Q(1,0)	Q(0,0)	B(0,0)	Q(1,0)	B bands	Q bands
SATltp	Acetone	444(4.553)	588(4.452)	603(4.218)	1319	432	0.0561	0.0568
	Chloroform	442(3.875)	588(4.230)	605(4.107)	1224	463	0.0413	0.0341
5-SSATltp	Acetone	445(4.553)	651(4.861)	649(4.434)	1591	647	0.0546	0.0534
	Chloroform	445(4.550)	651(4.332)	647(4.603)	1530	238	0.0623	0.0221
SATl(4-CH ₃)PP	Acetone	449(4.571)	572(4.243)	606(4.421)	1310	644	0.0431	0.0483
	Chloroform	447(3.571)	570(4.243)	605(4.314)	1227	425	0.2269	0.0322
5-SATl(4-CH ₃)PP	Acetone	451(4.043)	596(4.341)	673(4.210)	1398	565	0.2269	0.0404
	Chloroform	451(4.044)	594(4.235)	671(4.130)	1322	326	0.1342	0.0243
SATl(4-OCH ₃)PP	Acetone	435(4.670)	567(4.307)	611(4.313)	1354	683	0.2570	0.0600
	Chloroform	432(4.672)	566(4.302)	609(4.221)	1269	602	0.1725	0.0523
5-SATl(4-OCH ₃)PP	Acetone	449(4.747)	568(4.241)	671(4.04)	1373	588	0.3233	0.0591
	Chloroform	447(4.735)	568(4.113)	669(4.232)	1302	758	0.0869	0.0425

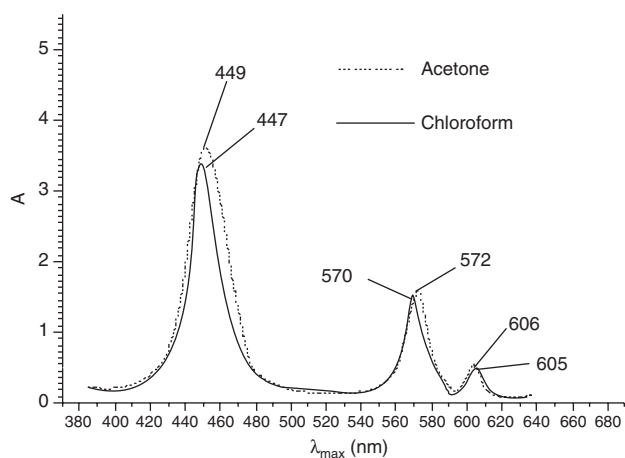


Figure 2: UV-visible overlapped B and Q bands of SATlt(4-CH₃)PP.

It is found that the $\nu(\text{N-H})$ stretching frequency of free base porphyrins are located at $\sim 3400\text{--}3320\text{ cm}^{-1}$ (Sun et al., 2011) and disappeared when thallium metal ion was inserted into the porphyrin ring. There is an additional Tl-N stretch vibration at $400\text{--}500\text{ cm}^{-1}$ in metalated complexes indicating the formation of Tl(III) porphyrins. The band in the complexes at 1633 cm^{-1} [$\nu_{\text{asymmetric}}(\text{OCO})$] are assigned to the chelating bidentate salicylate ligand. The bidentate nature of salicylates in the IR spectra of the complexes was confirmed on the basis of Stoilovo et al. results that unidentate CO_2 exhibits three bands (COO deformation) at $920\text{--}720\text{ cm}^{-1}$ and a strong band at 540 cm^{-1} (Suen et al., 1992). All these four bands were absent in axially ligated thallium porphyrin complexes. Further, the band observed near 1724 cm^{-1} is assigned to $\nu(\text{C=O})$ stretching frequency. The frequency corresponding to free O-H group is observed at 3418 cm^{-1} confirming the coordination of axial ligand through carboxylate oxygen atoms. The decrease in vibrational frequency of OH group is due to the weakening of O-H bond as $-\text{CO}_2$ in its vicinity from salicylate ring ligates to the metal atom.

¹H NMR spectroscopy

The thallium porphyrin complexes with salicylates (SA/5-SSA) as axial ligands all exhibit sharp ¹H NMR spectra. The characteristic data for the NMR of the free base porphyrins, corresponding metalated complexes of thallium(III) and their axially ligated derivatives are summarized in Table 5.

¹H NMR spectra are fruitful in clarifying the insertion of metal ion in the porphyrin core as the signal related to N-H protons was found to be absent, and also there was a shift in the signals of other protons in the NMR spectra of metalated porphyrins. In the axially ligated derivatives of thallium porphyrins, the singlet at 5.0 ppm of medium intensity was observed assigned to the -OH group which confirms that axial ligation was taking place through the oxygen atom of carboxylate group. All the δ values correspond to the proton signals of axial ligands in the axially ligated complexes that exhibited upfield shift when compared with the signals of porphyrin protons and the proton signal of free axial ligands. This upfield shift is attributed to the ring current effect (Lu et al., 1999) of the porphyrin macrocycle.

²⁰⁵Tl NMR spectroscopy

The range for ²⁰⁵Tl NMR chemical shift values is very large, i.e. about 7000 ppm. As far as oxidation states are concerned, for Tl(I) complexes chemical shift values are in the range -200 to $+200$ ppm, and for Tl(III) these lie in the range $+2000$ to $+3000$ ppm. ²⁰⁵Tl NMR spectra of SATl(III) t(4-CH₃)PP when recorded in CDCl_3 exhibits a sharp resonance at $\delta 2588$ ppm which confirms the presence of Tl(III) ion in the complex. On comparing this value with the chemical shift value of the complexes already reported in literature (Ma et al., 2003), it was found that this value has

Table 4: Main infrared absorption frequencies corresponding to the simple porphyrin H₂tpp and various groups in XTlt(4-Y)PP (X=SA, 5-SSA) and (Y=-H, -CH₃, -OCH₃).

Porphyrin	$\nu(\text{O-H})$ (cm^{-1})	$\nu(\text{N-H})$ (cm^{-1})	$\nu(\text{C-H})_{\text{asym}}$ (cm^{-1})	$\nu(\text{sp}^3\text{-CH})$	$\nu(\text{C-H})_{\text{sym}}$	$\nu(\text{C-N})$ (cm^{-1})	$\nu(\text{C=C})$ (cm^{-1})	$\nu(\text{C=O})$	$\nu(\text{Tl-N})$ (cm^{-1})
H ₂ tpp		3425	–	–	2923	1353	1582	–	–
(OH)(H ₂ O)Tltpp	3523	–	–	–	2920	1351	1552	–	488
SATlt(4-H)PP	3419	–	2960	2854	2925	1328	1533	1725	472
5-SSATlt(4-H)PP	3401	–	2962	2859	2929	1336	1535	1728	470
SATlt(4-CH ₃)PP	3418	–	2960	2855	2919	1329	1534	1724	473
5-SSATlt(4-CH ₃)PP	3401	–	2962	2859	2929	1335	1533	1728	470
SATlt(4-OCH ₃)PP	3419	–	2960	2854	2925	1329	1532	1725	472
5-SSATlt(4-OCH ₃)PP	3401	–	2961	2859	2929	1336	1534	1728	472

Table 5: ^1H NMR data showing chemical shift (in ppm) values of axially ligated thallium porphyrins in CDCl_3 at 300 K.

Porphyrins	Pyrrole protons	Meso-aryl protons	Other protons
SATIt(4-H)PP	9.06 (s) 5.6 (d)	8.89s and 8.75s ($\text{H}_{2,6}$) 7.72s and 7.71s ($\text{H}_{3,5}$) 7.68m (H_4)	6.78t, $\text{H}_{4''}$ 6.08d, $\text{H}_{3''}$ 6.31d, $\text{H}_{6''}$ 6.16 t, $\text{H}_{5''}$, 5.0(s, 1H, O-H)
5-SSATIt(4-H)PP	8.78(s) 7.19(s), 5.6(dd)	8.15 and 8.06 (d, $\text{H}_{2,6}$) 7.99 and 7.78(d, $\text{H}_{2',6'}$) 7.7 (bs, $\text{H}_{3,5}$)	5.1–6.0m $\text{H}_{6''}$, $\text{H}_{4''}$, $\text{H}_{3''}$ 5.0(s, 1H, O-H) 2.0(bs, 1H, SO_3H)
SATIt(4- CH_3)PP	9.01(s) 5.5(d)	8.76s and 8.63s($\text{H}_{2,6}$) 7.63s and 7.61($\text{H}_{3,5}$)	6.78t, $\text{H}_{4''}$ 6.07d, $\text{H}_{3''}$ 6.29d, $\text{H}_{6''}$ 6.13t, $\text{H}_{5''}$, 5.0(s, 1H, O-H) 2.83(s, 12H, CH_3)
5-SSATIt(4- CH_3)PP	8.72(s) 7.14(s) 5.5(m)	8.02 and 7.98(d, $\text{H}_{2,6}$) 7.63 and 7.34(d, $\text{H}_{2',6'}$)	4.5–5.6m $\text{H}_{6''}$, $\text{H}_{4''}$, $\text{H}_{3''}$ 5.0(s, 1H, O-H), 2.0(bs, 1H, SO_3H), 2.83(s, 12, CH_3)
SATIt(4- OCH_3)PP	8.83(s) 5.5(m)	8.77 and 8.73(s, $\text{H}_{2,6}$) 7.62 and 7.59(s, $\text{H}_{3,5}$)	6.78t, $\text{H}_{4''}$ 6.06d, $\text{H}_{3''}$ 6.30d, $\text{H}_{6''}$ 6.11t, $\text{H}_{5''}$, 5.0(s, 1H, O-H) 4.15(s, 12H, OCH_3)
5-SSATIt(4- OCH_3)PP	8.69 and 7.14(s) 5.5(m)	7.83 and 7.13(d, $\text{H}_{2,6}$) 7.64–7.33(d, $\text{H}_{2',6'}$) 7.3(bs, $\text{H}_{3,5}$)	4.6–6.0m, $\text{H}_{6''}$, $\text{H}_{4''}$, $\text{H}_{3''}$ 5.0(s, 1H, O-H), 2.0(1s, 1H, SO_3H)

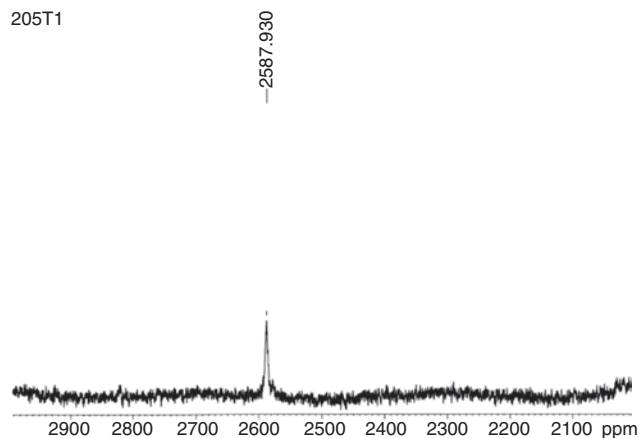
δ in ppm, the nature of splitting patterns(s) (s, singlet; d, doublet; m, multiplet; bs, broad singlet; dd, doublet of doublet; o, ortho; p, para; m, meta).

shifted towards lower frequency which can be attributed to the presence of four electron-releasing $-\text{CH}_3$ groups on the meso-phenyl ring. This parameter causes shielding of the thallium nucleus and hence shifts towards lower frequency (Figure 3).

Thermal analysis

The thermogravimetric (TG) curve of one of the synthesized complex 5-SSATl(III)t(4-H)pp (Figure 4) shows a continuous weight loss starting from 150°C to 750°C . The

curve shows an initial weight loss of a sulphosalicylate group and one phenyl ring at 158.2°C (obs. wt. loss=27.7%, calc. wt. loss=27.2%). This is followed by a loss of three phenyl rings and thallium metal ion at 408.5°C (obs. wt. loss=40.2%, calc. wt. loss=40.2%). There are some exothermic peaks observed in the range of 300 – 600°C showing major weight loss in this region. It is a continuous decomposition process; the small exothermic peaks correspond to the loss of chains of the porphyrin ring (Zhuang et al., 2009), and the large exothermic peaks at nearly 580°C corresponds to the collapse of the porphyrins skeleton. The residual mass was 0 at 751.2°C .

**Figure 3:** ^{205}Tl NMR spectrum of the complex SATIt(4- CH_3)PP.

Fluorescence spectroscopy

The variation of emission properties in free base porphyrin $\text{H}_2\text{t}(4\text{-Y})\text{PP}$ (Y: $-\text{CH}_3$, $-\text{OCH}_3$) and their axially ligated Tl(III) porphyrins have been investigated by means of fluorescence spectroscopy; data are given in Table 6. Porphyrins show two emission bands, a strong Q(0,0) band at higher energy accompanied by a weak Q(0,1) band at a lower energy. The free-base porphyrins $\text{H}_2\text{t}(4\text{-CH}_3)\text{PP}$, with excitation at 450nm, exhibits two emission bands at 620 and 672 nm corresponding to Q(0,0) and Q(0,1) transitions, respectively, the intensity of the Q(0,0) being higher than the Q(0,1) transition. Meso-substitution of the

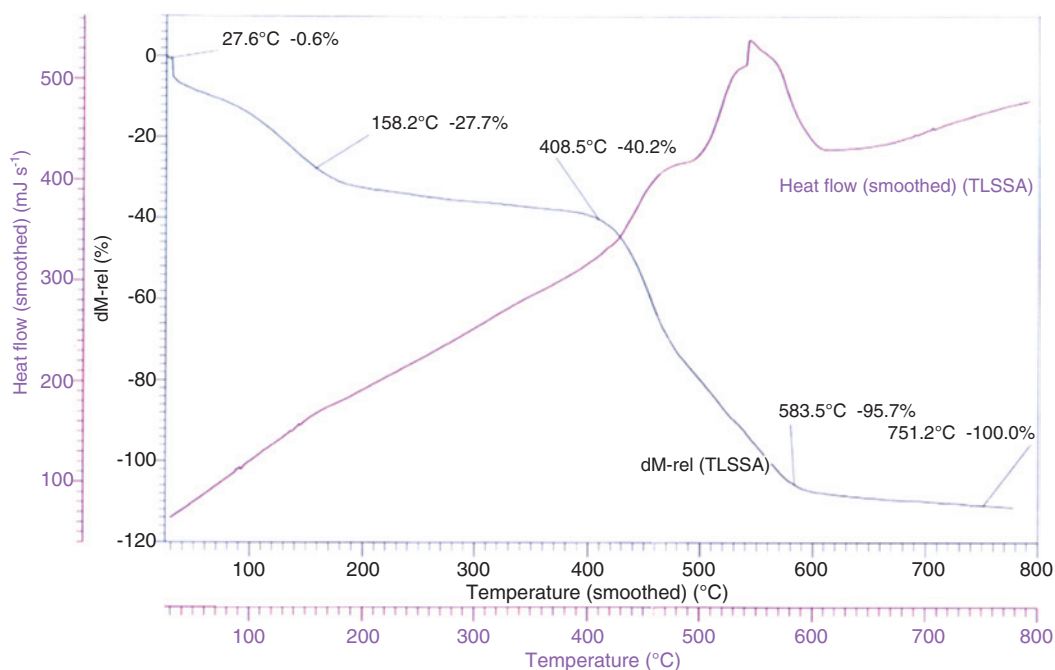


Figure 4: Thermogravimetric analysis (TGA)-differential thermal analysis (DTA) curve of 5-SSATltp.

Table 6: Summary of the characteristic emission data of free base porphyrin and axially ligated Tl(III) porphyrin at 28K in DMSO.

Complexes	λ_{\max} (nm)	
	Q(0,0)	Q(0,1)
H ₂ t(4-CH ₃)PP	620	672
Tlt(4-CH ₃)PP	606	653
SATlt(4-CH ₃)PP	580	630
H ₂ t(4-OCH ₃)PP	620	671
5-SSATlt(4-OCH ₃)PP	582	630

porphyrin ring leads to red shift of all the emission bands relative to that of unsubstituted tetraphenylporphyrins. However, the emission bands of axially ligated Tl(III) porphyrins are blue shifted (Horvath et al., 2006) compared to free base porphyrins. This behavior is attributed to an enhanced spin-orbit coupling induced by the presence of the heavy central metal atom in thallium porphyrin complexes, which leads to a more efficient $S_1 \rightarrow T_1$ intersystem crossing and thus reduces the probability of fluorescent emission (Knörra and Strasser, 2002). Thus, the excitation spectrum of fluorescence is in agreement with the absorption spectrum (Figure 5).

Mass spectrometry

The mass spectra of some of the investigated axially ligated thallium porphyrin complexes are characterized

by the presence of the molecular ion peak followed by different specific fragmentation pattern. The molecular ion peak of the investigated complexes was found to be 44 units less than the corresponding molecular weight of the complex, which is attributed to the loss of stable CO₂ molecule from the complex. The major losses are 304, 615, 616 and 81. Besides the molecular ion, an identical peak $m/z=304$ fragment, corresponding to the tetrapyrrole moiety, appears in each spectrum (Cosma et al., 2006). Two groups of peaks were observed (main signals accompanied by isotopic patterns confirming the chemical composition of the ions) at m/z 615 and 616 that correspond to the fragments of H₂tpp+1 and H₂tpp+2 (H₂tpp=meso-tetraphenyl porphyrin), and the peak at 81 corresponds to the SO₃H group.

In addition, the intensities of the registered peaks are significantly higher. The base peak of thallium porphyrin complexes was observed 100% intensity giving evidence about the stability of complexes of thallium porphyrins.

Antibacterial studies

Antibacterial activity of the synthesized Tl(III) porphyrin complexes was tested by agar well diffusion method. The free base porphyrins, their corresponding metalated and axially ligated thallium(III) porphyrin complexes viz., H₂t(4-OCH₃)PP, H₂t(4-CH₃)PP, (OH)(H₂O)Tlt(4-CH₃)PP, (OH)(H₂O)Tlt(4-OCH₃)PP, SATlt(4-CH₃)PP, 5-SSATlt(4-CH₃)PP

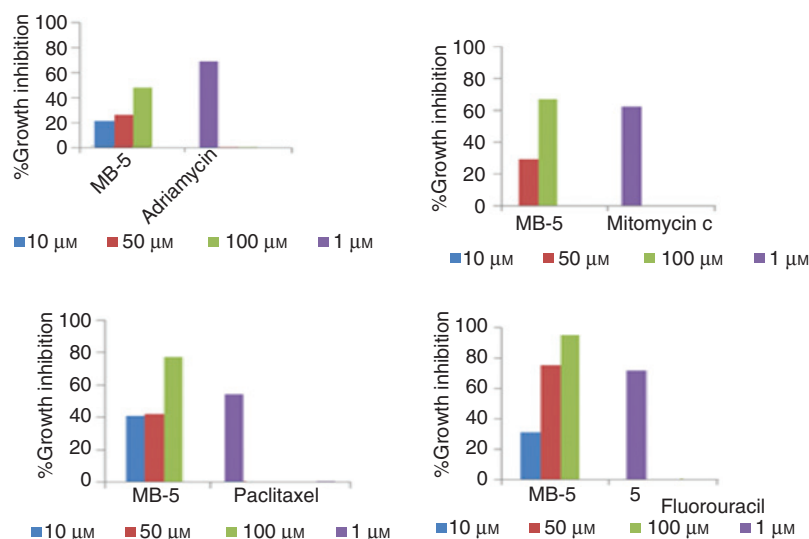


Figure 5: *In vitro* cytotoxicity of 5-SSATt(4-OCH₃)PP complex against human cancer cell lines.

and 5-SSATt(4-OCH₃)PP were tested at three concentrations (10^{-3} , 10^{-4} and 10^{-5} M) against five bacterial strains *viz.*, *B. subtilis*, *Micrococcus luteus*, *S. aureus*, *Pseudomonas fluorescens* and *E. coli*. The thallium(III) complex 5-SSATt(4-OCH₃)PP was found sensitive only to *B. subtilis* (Gram positive) and *P. fluorescens* (Gram negative) bacteria at the concentrations of 10^{-3} and 10^{-4} M. Other complex SATt(4-CH₃)PP showed sensitivity against *B. subtilis* and *M. luteus*. The remaining complexes, *viz.*, H₂t(4-CH₃)PP, (OH)(H₂O)Tt(4-CH₃)PP and 5-SSATt(4-CH₃)PP showed activity only against Gram negative bacteria *E. coli* with zone of inhibition ranging from 6 to 14 mm. The rest of the complexes did not show any activity against bacterial strains. The results were observed in dose-dependent manner as demonstrated in Table 7.

Anticancer activity

In the present work, the cytotoxicities of 5-SSAT(III)t(4-OCH₃)PP, SAT(III)t(4-OCH₃)PP and SAT(III)t(4-CH₃)PP were evaluated against four human cancer cell lines, *viz.*, breast (MCF-7), leukemia (THP-1), prostate (PC-3) and lung (A549) at different concentrations. One of the complexes, namely, 5-Sulphosalicylato (meso-tetra-p-methoxy porphyrinato)thallium(III) (MB-5) shows significant activity (Figure 5) against lung and leukemia, classifying these complexes as chemotherapeutically significant. We also tested other synthesized compounds against the above mentioned panel of cancer cell lines; however, none of the compounds exhibited cytotoxicity even at 100 μM concentration (results not shown).

Conclusion

The present paper was concerned about the synthesis of symmetrically substituted meso-tetraphenylporphyrin, their complexation with thallium metal ion and then axial ligation with salicylates, SA/5-SSA. The complexes were characterized by elemental analysis, UV-Vis, IR, fluorescence and NMR studies. In the UV-Vis spectra, both the Soret and Q bands were significantly red shifted on metalation, and further large shift of these bands on axial ligation was related to the distortion of the porphyrin core. The IR spectrum of these compounds showed that salicylic acids (SA/5-SSA) ligate in a bidentate mode through the carboxylate group. ¹H NMR spectroscopic study of these compounds showed that due to ring current effect of the porphyrin macrocycle, the proton signals of the axial ligands (SA/5-SSA) are shifted to higher field in comparison to the signals of porphyrin protons and proton signals of free axial ligands. The production of the monomeric form of thallium porphyrin complexes was well confirmed by means of electrospray ionization mass spectrometry (ESI-MS). The coordination of salicylates through COO to these complexes in methanol solution was clarified using ESI-MS. The ensuing complexes show admirable thermal stability (>400°C), and the decomposition of the complexes comes to an end at 750°C. ²⁰⁵Tl NMR studies confirm the presence of Tl(III) ion in the complexes. The biological activities were also investigated, and the synthesized compounds showed varying degrees of inhibitory effects: low (up to 6 mm) and moderate (up to 11 mm). The parent compounds possessed a low activity against the bacterial strains at low concentration but indicated a slight rise in the activity at 100 μg mL⁻¹. Similarly,

Table 7: *In vitro* antibacterial evaluation of free base porphyrin and the corresponding thallium porphyrin complexes.

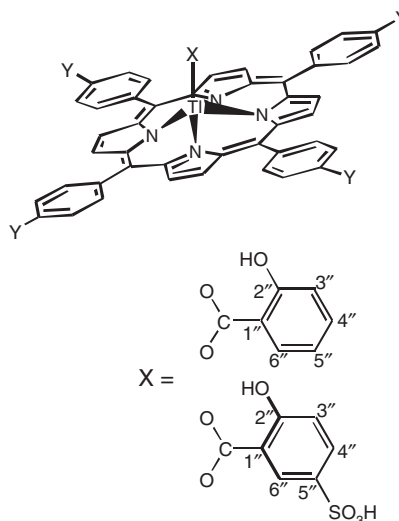
Bacterial strains	Conc.	<i>B. subtilis</i>	<i>M. luteus</i>	<i>S. aureus</i>	<i>P. fluorescens</i>	<i>E. coli</i>
Zones of inhibition (mm)						
$H_2t(4-OCH_3)PP$	10^{-3}					8
	10^{-4}					6
	10^{-5}					–
SATIt(4- OCH_3)PP	10^{-3}		9		6	
	10^{-4}		7		–	
	10^{-5}		–		–	
5-SSATIt(4- OCH_3)PP	10^{-3}	10			8	
	10^{-4}	6			6	
	10^{-5}	–			–	
$H_2t(4-CH_3)PP$	10^{-3}					6
	10^{-4}					4
	10^{-5}					–
(OH)(H_2O)TIt(4- CH_3)PP	10^{-3}					9
	10^{-4}					6
	10^{-5}					–
SATIt(4- CH_3)PP	10^{-3}	7	9		10	9
	10^{-4}	–	6			
	10^{-5}	–	–			
5-SSATIt(4- CH_3)PP	10^{-3}	9	9		10	10
	10^{-4}	–	–		–	–
	10^{-5}	–	–		–	–
Positive control		19	20	21	18	24
Control						
Cmp ⁺ 10 μ g						

thallium porphyrins and their axially ligated derivatives show rise in the activity when compared with their parent compounds. Such increase in the activity of the complexes compared to that of ligands could be explained on the basis of Overton's concept (Overton, 1901) and Tweedy's chelation theory (Tweedy, 1964). One of the complexes screened for anticancer activity showed up to 90% growth inhibition. On the basis of the elemental analysis and spectral studies, confirmed by mass spectra showing characteristic molecular ion peak at their m/z value for their monomeric form, a square-pyramidal structure (Figure 6) for SATI(III)t(4-Y)PP and 5-SSATIt(4-Y)PP complexes has been proposed. All complexes are soluble in DMSO, $CHCl_3$ and CH_3OH .

Experimental

Materials and instrumentation

All the chemicals were of analytical grade and were used as received unless otherwise noted. All the reagents were purchased from Himedia (Mumbai, India). Pyrrole was distilled over potassium hydroxide pellets under vacuum prior to use. All the organic solvents that were used for the synthesis and for chromatographic separations were dried before use. Elemental analysis (C, H, N and S) was performed on a Vario EL III and CHNS-932 LECO Elemental Analyzer (IIIM, Jammu).

**Figure 6:** Suggested structure of XTIt(4-Y)PP (X=SA, 5-SSA).

UV-Vis spectra were recorded on a Sytonic 119 UV Visible spectrophotometer (University of Jammu, Jammu) in the range 350–700 nm. The oscillator strength (f) of the transitions in absorption spectra were calculated from the expression

$$f = 4.33 \times 10^{-9} \epsilon \Delta \nu_{1/2}$$

where ϵ is the molar absorption coefficient in $dm^3 mol^{-1} cm^{-1}$ and $\Delta \nu_{1/2}$ is the fwhm in cm^{-1} . IR spectra were recorded on a Perkin

Elmer-spectrum 400 FTIR spectrophotometer using KBr pellets in the range of 4000–400 cm^{-1} . The ^1H NMR spectra were recorded on a Bruker Avance II 500 (500 MHz) using tetramethylsilane as internal standard and CDCl_3 as solvent. ^{205}Tl NMR spectra were recorded on a Bruker Avance 400 MHz spectrometer in CDCl_3 . TGA and DTA were recorded on Linseis STA PT-100 thermometer using dry samples at the heating rate of $10^\circ\text{C min}^{-1}$ in an air atmosphere. Fluorescence measurements were performed on Synergy MX BIOTEK Multimode Reader. The porphyrin solution prepared in CH_2Cl_2 was 10^{-6} M.

Biological studies

Antibacterial studies: Qualitative analysis for screening of antimicrobial activity of the complexes was carried out by agar well diffusion method with modifications. The complexes were tested against two Gram positive bacteria (*B. subtilis* MTCC2389 and *S. aureus* MTCC7443) and three Gram negative bacteria (*M. luteus* MTCC4821, *E. coli* MTCC2127 and *P. fluorescens* MTCC4828). Twenty milliliters of sterilized nutrient agar were inoculated with 100 mL of bacterial suspension (10^8 CFU mL^{-1}) and then poured on to sterilized petri plate. The agar plate was left to solidify at room temperature. A well of 6 mm was aseptically bored into the agar plate. Then 20 mL of the complexes (diluted with DMSO, 1:1) was added in each well. Chloramphenicol (10 μg) was used as a positive reference to determine the sensitivity of bacteria. The plates were kept at 4°C for 2 h to allow the dispersal and then incubated at 37°C for 24 h.

In vitro cytotoxicity against human cancer cell lines

Cell lines and cell cultures: The human prostate (PC-3), lung (A-549) and acute lymphoblastic leukemia (THP-1) cell lines were grown and maintained in RPMI-1640 medium, pH 7.4, whereas DMEM was used for breast (MCF-7). The media were supplemented with FCS (10%), penicillin (100 units mL^{-1}), streptomycin (100 $\mu\text{g mL}^{-1}$) and glutamine (2 mM), and cells were grown in CO_2 incubator (Heraeus, GmbH, Germany) at 37°C with 90% humidity and 5% CO_2 . Cells were treated with samples dissolved in DMSO, while the untreated control cultures received only the vehicle (DMSO, <0.2%).

Cytotoxicity assay

In vitro cytotoxicity against human cancer cell lines was determined using sulphorhodamine B dye assay (Thiantanawat et al., 2003; Tong et al., 2004). Both test sample stock solutions were prepared in DMSO and serially diluted with growth medium to obtain desired concentrations.

Synthesis of axially ligated thallium(III) porphyrin complexes

Synthesis of macrocycles

H_2tPP and $\text{H}_2\text{t}(4\text{-Y})\text{TPP}$ ($\text{Y} = -\text{CH}_3$ and $-\text{OCH}_3$) were synthesized. The synthesis of the porphyrins has been adapted

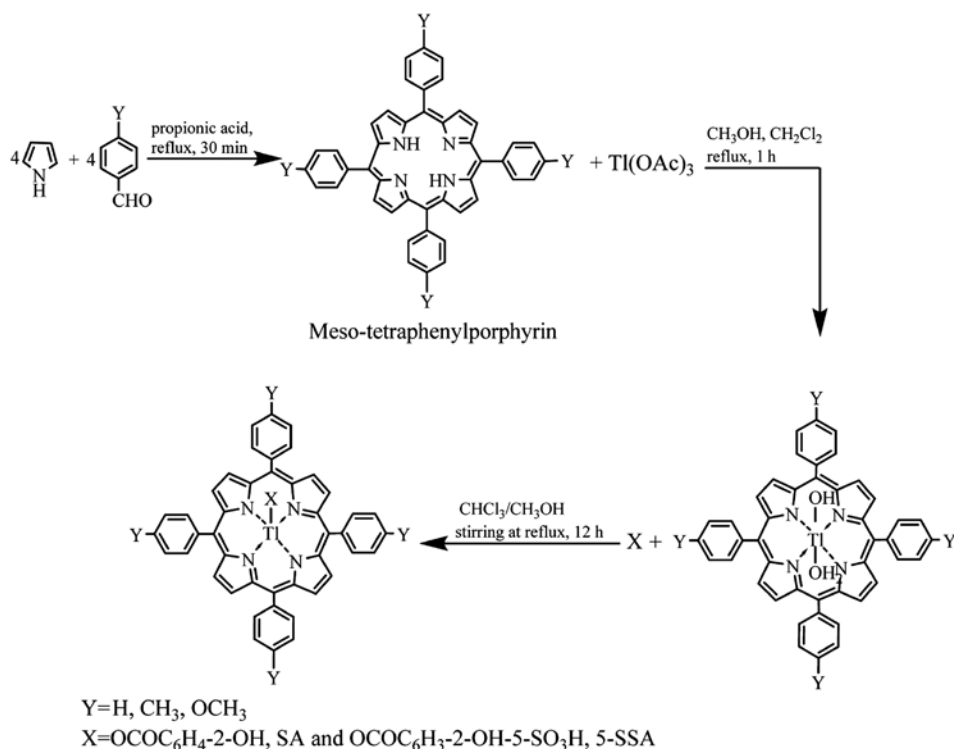
from the synthesis reported by Adler et al. (1967). The appropriate benzaldehyde is refluxed for 30 min with 0.08 mL of pyrrole in 12 mL of propionic acid in a 50-mL round bottom flask fitted with a water condenser. The pyrrole must be from a freshly opened bottle or have recently been purified by vacuum distillation. After refluxing, the reaction mixture is cooled to room temperature, and 10 mL of cold methanol is added. The deep-purple solid is filtered by vacuum filtration with a Buchner funnel. The flask and crude solid is washed with three portions of cold methanol followed by boiling distilled water. The crystals are air-dried on the Buchner funnel for 15 min, dried in a vacuum desiccator and purified by column chromatography (Scheme 1). The syntheses of the substituted porphyrins, i.e. $\text{H}_2\text{t}(4\text{-CH}_3)\text{TPP}$ and $\text{H}_2\text{t}(4\text{-OCH}_3)\text{TPP}$, are performed in a similar manner. Average yields are about 40 mg (23%). All the benzaldehydes are commercially available. The resulting porphyrins can be characterized by visible absorption or ^1H NMR spectroscopy.

Synthesis of aquo-meso-(5,10,15,20-tetraarylporphyrinato)thallium(III) hydroxide, $[(\text{OH})(\text{H}_2\text{O})\text{Tltp}]$ and $(\text{OH})(\text{H}_2\text{O})\text{Tl}(\text{4-Y})\text{PP}$ ($\text{Y} = -\text{CH}_3, -\text{OCH}_3$)

A mixture of meso-tetraphenylporphyrins 0.0068 mmol in CH_2Cl_2 (10 mL) and $\text{Tl}(\text{OAc})_3$ 0.12 mmol in MeOH (2.5 mL) was refluxed for 1 h. After concentration, the residue was dissolved in CHCl_3 , dried with anhydrous Na_2SO_4 and filtered. The filtrate was concentrated and recrystallized from CH_2Cl_2 -MeOH (1:5 v/v) yielding purple solid of complex, (0.037 mmol, 55%), which was again dissolved in CH_2Cl_2 -ether [1:1 (v/v)] and layered with MeOH to get purple crystals of thallium(III) porphyrins (Scheme 1).

Synthesis of axially ligated Tl(III) Porphyrins: $\text{Tl}(\text{4-Y})\text{PP}$, SA and $\text{Tl}(\text{4-Y})\text{PP}$, 5-SSA

$(\text{OH})(\text{H}_2\text{O})\text{Tl}(\text{III})\text{t}(4\text{-Y})\text{PP}$ 0.15 mmol in 30 mL CHCl_3 was treated with respective salicylates 0.56 mmol in 25 mL CH_3OH and stirred under reflux for 12 h. After concentration, the mixture was dissolved in minimum quantity of CH_2Cl_2 and extracted four times with distilled water to remove excess unreacted salicylates (SA, 5-SSA). The resulting solution was then filtered through anhydrous Na_2SO_4 in order to remove water molecule. The CH_2Cl_2 layer was then concentrated to dryness, producing purple prism. The same procedure was applied for the



Scheme 1: Synthesis of meso-tetraphenylporphyrins and their corresponding metalated and axially ligated derivatives.

synthesis of all axially ligated complexes of thallium porphyrins. The overall route for the synthesis of axially ligated thallium (III) porphyrin complexes is given in Scheme 1.

Acknowledgments: We thank Department of Chemistry and Department of Biotechnology, University of Jammu, IIIM Jammu, IISc Bangalore, India for providing support.

References

- Adler, A. D.; Longo, F. R.; Finarelli, J. D.; Goldmacher, J.; Assour, J.; Korsakoff, L. A simplified synthesis for meso-tetraphenylporphyrine. *J. Org. Chem.* **1967**, *32*, 476–476.
- Antonova, N. A.; Osipova, V. P.; Kolyada, M. N.; Movchan, N. O.; Milaeva, E. R.; Pimenov, Y. T. Study of the antioxidant properties of porphyrins and their complexes with metals. *Macromolecules* **2010**, *3*, 139–144.
- Cosma, F. G.; Badea, V.; Vlascici, D.; Cosma, F.-E.; Simon, M. The 13th Symposium on Analytical and Environmental Problems, Szeged. **2006**, 84–87.
- Cosma, E. F.; Mirica, M. C.; Balcu, I.; Bucovician, C.; Cretu, C.; Armeanu, I.; Cosma, G. F. Syntheses, spectroscopic and AFM characterization of some manganese porphyrins and their hybrid silica nanomaterials. *Molecules* **2009**, *14*, 1370–1388.
- Drain, C. M.; Hupp, J. T.; Suslick, K. S.; Wasielewski, M. R.; Chen, X. A perspective on four new porphyrin-based functional materials and devices. *J. Porphy. Phthal.* **2002**, *6*, 243–258.
- Fadda, A. A.; El-Mekawy, R. E.; El-Shafei, A.; Freeman, H. S.; Hinks, D.; El-Fedawy, M. Design, synthesis, and pharmacological screening of novel porphyrin derivatives. *J. Chem.* **2013**, *2013*, 11.
- Fitzgerald, J. P.; Huffman, P. D.; Brenner, I. A.; Wathen, J. J.; Beadie, G.; Pong, R. G. S.; Shirk, J. S.; Flom, S. R. Synthesis, chemical characterization and nonlinear optical properties of thallium(III) phthalocyanine halide complexes. *Opt. Mater. Express.* **2015**, *5*, 19.
- Horvath, O.; Valicsek, Z.; Vogler, A. Unique photoreactivity of mercury (II) 5,10,15,20-tetrakis (4-sulfonatophenyl)porphyrins. *Inorg. Chem. Commun.* **2004**, *7*, 854–857.
- Horvath, O.; Huszank, R.; Valicsek, Z.; Lendvay, G. Photophysics and photochemistry of kinetically labile, water-soluble porphyrin complexes. *Coord. Chem. Rev.* **2006**, *250*, 1792–1803.
- Karimipour, G.; Karami B.; Montazerzohori M.; Zakavi S. Oxidative decarboxylation of carboxylic acids with tetrabutylammonium periodate catalyzed by manganese (III) meso-tetraarylporphyrins: effect of metals, meso-substituents, and anionic axial ligands. *Chinese J. Catal.* **2007**, *28*, 940–946.
- Karimipour, G.; Ghaedi, M.; Behfar, M.; Andikaey, Z.; Kowkabi, S.; Orojloo, A. H. Synthesis and application of new porphyrin derivatives for preparation of copper selective electrodes: influence of carbon nanotube on their responses. *IEEE Sens. J.* **2012**, *12*, 2638–2647.
- Karimipour, G.; Rezaei M.; Ashouri D. Zeolite encapsulated Fe-porphyrin for catalytic oxidation with iodobenzene diacetate (PhI(OAc)₂). *J. Mex. Chem. Soc.* **2013**, *57*, 276–282.
- Knörra, G.; Strasser, A. Coexisting intraligand fluorescence and phosphorescence of hafnium(IV) and thorium(IV) porphyrin complexes in solution. *Inorg. Chem. Commun.* **2002**, *5*, 993–995.

- Lu, Y. Y.; Tung, J. Y.; Chen, J. H.; Liao, F. L.; Wang, S. L.; Wang, S. S.; Hwang, L. P. Salicylate exchange in meso-tetraphenylporphyrinato salicylate thallium (III), Tl (tpp) (2-OH-C₆H₄CO₂) and ¹³C NMR investigation of its homolog thiocyanato (meso-tetra-p-tolylporphyrinato)thallium(III), Tl (tptp)(SCN). *Polyhedron*. **1999**, *1*, 145–150.
- Ma, G.; Fischer, A.; Ilyukhin, A.; Glaser, J. Formation and structure of novel ternary complexes of thallium(III)-cyanide–amine (ethylenediamine and triethylenetetramine) in solution and in solid. *Inorg. Chim. Acta*. **2003**, *344*, 117–122.
- Manke, A. M.; Geisel, K.; Fetzner, A.; Kurz, P. A water-soluble tin(IV) porphyrin as a bioinspired photosensitizer for light-driven proton-reduction. *Phys. Chem. Chem. Phys.* **2014**, *16*, 12029–12042.
- Milgrom, L. R. *The Colors of Life, an Introduction to the Chemistry of Porphyrins and Related Compounds*. Oxford University Press: Oxford, **1997**.
- Musturappa, P. K.; Reddy, V. K. R.; Kotresh, H. M. N.; Basappa, C.; Jayanna, M. B.; Devendrachari, M. C.; Fasiulla. New metallophthalocyanines posture pyridine pendants via 1,3,4-oxadiazole bridge: synthesis, optical and electrical studies. *Chem. Sci. J.* **2013**, *2013*, 11.
- Overton CE. Studien uber die Narkose zugleich ein Beitrag zur allgemeinen Pharmakology. Gustav Fisher, Jena: Switzerland, **1901**.
- Rajesh, K.; Rahiman, A. K.; Bharathi, K. S.; Sreedaran, S.; Gan-gadevi, V.; Narayanan, V. Spectroscopic, redox and biological studies of push-pull porphyrins and their metal complexes. *B. Kor. Chem. Soc.* **2010**, *31*, 2656–2664.
- Stojiljkovic, I.; Evavold, B. D.; Kumar, V. Antimicrobial properties of porphyrins. *Expert Opin. Invest. Drugs*. **2001**, *10*, 309–320.
- Suen, S. C.; Lee, W. B.; Hong, F. E.; Jong, T. T.; Chen, J. H. Molecular structure of thallium (III) meso-tetraphenylporphyrin acetate Tltpp(OAc). *Polyhedron*. **1992**, *11*, 3025–3030.
- Sun, Z.-C.; She, Y.-B.; Zhou, Y.; Song, X.-F.; Li, K. Synthesis, characterization and spectral properties of substituted tetraphenylporphyrin iron chloride complexes. *Molecules*. **2011**, *16*, 2960–2970.
- Thiantanawat, A.; Long, B. J.; Bordie, A. M. Signaling pathways of apoptosis activated by aromatase inhibitors and antiestrogens. *Cancer Res.* **2003**, *63*, 8037–8050.
- Tong, X.; Lin, S.; Fujii, M.; Hou, D. X. Erratum to Echinocystic acid induces apoptosis in HL-60 cells through mitochondria-mediated death pathway. *Cancer Lett.* **2004**, *212*, 21–32.
- Tweedy, B. G. Plant extracts with metal ions as potential antimicrobial agents. *Phytopathology*. **1964**, *55*, 910–917.
- Valicsek, Z.; Horvath O.; Stevenson, K. L. Photophysics and photochemistry of water-soluble, sitting-atop bis-thallium(I) 5,10,15,20-tetrakis(4-sulfonatophenyl)porphyrin. *Photochem. Photobiol. Sci.* **2004**, *3*, 669–673.
- Valicsek, Z.; Horvath, O.; Lendvay, G.; Kikas, I.; Skoric, I. Formation, photophysics, and photochemistry of cadmium(II) complexes with 5,10,15,20-tetrakis(4-sulfonatophenyl) porphyrin and its octabromo derivative: The effects of bromination and the axial hydroxo ligand. *J. Photoch. Photobio. A.* **2011**, *218*, 143–155.
- Yuasa, M.; Oyaizu, K.; Murata, H.; Sahara, Y.; Hatsugai, T.; Ogata, A. Antioxidant and anticancer properties of metalloporphyrins embedded in liposomes. *J. Oleo Sci.* **2007**, *56*, 87–93.
- Zhuang, C.; Tang, X.; Wang, D.; Xia, A.; Lian, W.; Shi, Y.; Shi, T. An unsymmetrical porphyrin and its metal complexes: synthesis, spectroscopy, thermal analysis and liquid crystal properties. *J. Serb. Chem. Soc.* **2009**, *74*, 10.